



FULL LENGTH ARTICLE

# Genetic profiles of familial late-onset Alzheimer's disease in China: The Shanghai FLOAD study

Xin-Yi Xie <sup>a,2</sup>, Qian-Hua Zhao <sup>b,c,2</sup>, Qiang Huang <sup>a</sup>,  
Eric Dammer <sup>d</sup>, Sheng-di Chen <sup>a</sup>, Ru-Jing Ren <sup>a,\*\*</sup>,  
Gang Wang <sup>a,\*</sup>, the Alzheimer's Disease Neuroimaging Initiative <sup>1</sup>

<sup>a</sup> Department of Neurology and Institute of Neurology, Ruijin Hospital Affiliated with Shanghai Jiao Tong University School of Medicine, Shanghai 200025, PR China

<sup>b</sup> Institute of Neurology, Huashan Hospital, Fudan University, Shanghai 200040, PR China

<sup>c</sup> National Clinical Research Center for Aging and Medicine, Huashan Hospital, Fudan University, Shanghai 200040, PR China

<sup>d</sup> Department of Biochemistry, Center for Neurodegenerative Disease, Emory University School of Medicine, Atlanta, GA 30322, USA

Received 28 April 2021; received in revised form 21 May 2021; accepted 24 May 2021

Available online 1 June 2021

## KEYWORDS

ACE;  
Alzheimer's disease;  
Familial late-onset  
Alzheimer's disease;  
Gene;  
Mutation

**Abstract** Compared with early-onset familial AD (FAD), the heritability of most familial late-onset Alzheimer's disease (FLOAD) cases still remains unclear. However, there are few reported genetic profiles of FLOAD to date. In the present study, targeted sequencing of selected candidate genes was conducted for each of 90 probands with FLOAD and 101 unrelated matched normal controls among Chinese Han population. Results show a significantly lower rate of mutation in APP and PSENs, and APOE  $\epsilon$ 4 genetic risk is higher for FLOAD. Among the Chinese FLOAD population, the most frequent variant was CR1 rs116806486 [5.6%, 95% CI (1.8%, 12.5%)], followed by coding variants of TREM2 (4.4%, 95%CI (1.2%, 10.9%)) and novel mutations of ACE [3.3%, 95%CI (0.7%, 9.4%)]. Next, we found that novel pathogenic mutations in

\* Corresponding author. Fax: +021 64454473.

\*\* Corresponding author.

E-mail addresses: [doctorren2001@163.com](mailto:doctorren2001@163.com) (R.-J. Ren), [wgneuron@hotmail.com](mailto:wgneuron@hotmail.com) (G. Wang).

Peer review under responsibility of Chongqing Medical University.

<sup>1</sup> Some data used in preparation of this article were obtained from the Alzheimer's Disease Neuroimaging Initiative (ADNI) database ([adni.loni.usc.edu](http://adni.loni.usc.edu)). As such, the investigators within the ADNI contributed to the design and implementation of ADNI and/or provided data but did not participate in analysis or writing of this report. A complete listing of ADNI investigators can be found at: [http://adni.loni.usc.edu/wp-content/uploads/how\\_to\\_apply/ADNI\\_Acknowledgement\\_List.pdf](http://adni.loni.usc.edu/wp-content/uploads/how_to_apply/ADNI_Acknowledgement_List.pdf).

<sup>2</sup> These authors contributed equally to this work.

*ACE* including frame-shift and nonsense mutations were in association with FLOAD regardless of *APOE*  $\epsilon 4$  status. Evidence from the Alzheimer's disease Neuroimaging Initiative (ADNI) database also supported this finding in different ethnicities. Results of *in vitro* analysis suggest that frame-shift and nonsense mutations in *ACE* may be involved in LOAD through decreased *ACE* protein levels without affecting direct processing of APP.

Copyright © 2021, Chongqing Medical University. Production and hosting by Elsevier B.V. This is an open access article under the CC BY-NC-ND license (<http://creativecommons.org/licenses/by-nc-nd/4.0/>).

## Introduction

The most common form of dementia, Alzheimer's disease (AD), is divided into early-onset AD (EOAD) and late-onset AD (LOAD) according to the age at onset, with 60 or 65 years as the boundary, usually. In addition to memory impairment, atypical clinical manifestations such as visual space disorder, apraxia, dyscalculia, aphasia, and executive dysfunction are more common in the early stage of EOAD.<sup>1,2</sup> Simultaneously, AD can also be separated into familial AD (FAD) and sporadic AD in terms of family history. Interestingly, genetic backgrounds differ between familial EOAD and familial LOAD (FLOAD). Mutations in genes encoding amyloid precursor protein (APP [OMIM: 104760]), presenilin 1 (PSEN1 [OMIM: 104311]) and presenilin 2 (PSEN2 [OMIM: 600759]), which all lead to  $A\beta$  overproduction, account for about 10%–20% of familial AD, especially familial EOAD.<sup>3–5</sup> Meanwhile, the Apolipoprotein E (*APOE* [OMIM: 107741])  $\epsilon 4$  allele is the most powerful genetic risk factor identified for LOAD.<sup>6,7</sup> Increased risks for AD are estimated to 2–4 folds with a single  $\epsilon 4$  allele, whereas 8–16 folds with two  $\epsilon 4$  alleles.<sup>8,9</sup> Unfortunately, the majority of heritable risk for FAD remains an open question.

In recent years, whole-genome/whole-exome sequencing technology and data analysis based on large sample sizes have found a series of coding mutations in *ADAM10* [OMIM: 602192],<sup>10</sup> *TREM2* [OMIM: 605086],<sup>11,12</sup> and *PLD3* [OMIM: 615698]<sup>13</sup> increase the risk of AD. Genome-wide association studies (GWAS) have discovered more than 20 risk genes for AD,<sup>14,15</sup> involving immunity, metabolism, endocytosis, APP and tau metabolism, and other pathways. Generally, GWAS can only identify correlations between common variants with lower impact on risk for AD, but cannot determine rare coding variants with high pathogenicity. While, some studies choose FAD as the research object, the results are partly consistent with studies of sporadic AD. *ADAM10* and *PLD3* (mentioned above) were also found in LOAD pedigrees. *BIN1* [OMIM: 601248], *CLU* [OMIM: 185430]<sup>16</sup>; *CR1* [OMIM: 120620], *PICALM* [OMIM: 104760], *APOE*, *ADAM10*, *ACE* [OMIM: 106180]<sup>17</sup>; *PTK2B* [OMIM: 601212]<sup>18</sup>; and *TREM2*<sup>19</sup> have also been verified in GWAS analysis of LOAD populations with family history.

However, previous studies of FAD and disease-causing gene mutations mainly focus on familial EOAD and APP, PSEN1, along with PSEN2. Less is known regarding FLOAD. Based on previous studies mentioned above, we selected 13 candidate genes (*APP*, *PSEN1*, *PSEN2*, *ADAM10*, *TREM2*, *PLD3*, *BIN1*, *CLU*, *CR1*, *PICALM*, *APOE*, *ACE*, and *PTK2B*) which were detected not only in sporadic LOAD cohorts, but also verified in FAD cohorts, and we further performed

target enrichment sequencing in the Shanghai FLOAD cohort to reveal the genetic profiles of FLOAD in Chinese population.

## Material and methods

### Participants and clinical neuropsychological assessments

Probands of unrelated LOAD families were recruited from the Memory Clinic in Ruijin Hospital affiliated with Shanghai Jiaotong University School of Medicine and Huashan Hospital affiliated with Fudan University, respectively. All individuals were diagnosed with probable AD dementia<sup>20</sup> according to recommendations of the National Institute on Aging-Alzheimer's Association workgroups (NIA-AA). Additionally, AD-diagnoses met the following inclusion criteria: (1) persons of Chinese Han ethnicity, (2) > 60 years old, (3) with a family history, i.e., at least one first-degree relative suffering from dementia with a probable cause of LOAD. Individuals who had difficulty cooperating with neuropsychological assessments due to severe visual or hearing impairments were excluded. Unrelated elderly individuals with normal cognition who did not possess a family history of dementia were selected from an urban community in Shanghai as the control cohort. Scales of Mini-mental State Examination (MMSE) and Clinical Dementia Rating (CDR) cognitive assessments were performed for each participant. Montreal Cognitive Assessment (MoCA) and Addenbrooke's Cognitive Examination (ACE-III) were used in the probands if necessary. This study was approved by the Ethics Committee of Ruijin Hospital affiliated to Shanghai Jiaotong University School of Medicine and informed consent was obtained from all participants.

### Target enrichment sequencing and mutation analysis

We extracted DNA from about 3 ml of peripheral blood samples, which were collected from each participant. After quality examination of each sample, a total of 451 targets of the 13 candidate genes were enriched based on multiplex polymerase chain reactions (Genesky Biotechnologies Inc, Shanghai, China). High-throughput sequencing was performed on an Illumina HiSeq (Illumina, CA, USA). Clean reads were aligned to the reference genome by means of software employing the BWA algorithm<sup>21</sup> after quality control of raw data. The GATK<sup>22</sup> standard procedure was adopted to correct original alignment results and detect

single nucleotide variants (SNVs) and insertions or deletions (InDels). All SNV/InDel positions were annotated by ANNOVAR<sup>23</sup> to assess variant frequency, gene function, pathogenicity prediction, etc. The population database mainly referred to the Genome Aggregation Database (gnomAD) and hazard prediction referred to evidence from online tools (SIFT, POLYPHEN, Mutation Taster, and CADD). Missense variants of *APP*, *PSEN1*, *PSEN2*, and *TREM2* were also checked on the AlzForum database (<https://www.alzforum.org/mutations>) and defined as a novel mutation if neither recorded in AlzForum nor peer-reviewed publications.

Variants meeting one of the following conditions were selected out for Sanger sequencing verification: (1) defined as 'pathogenic' or 'likely pathogenic' according to the guidelines issued by the American College of Medical Genetics (ACMG)<sup>24</sup>; (2) non-synonymous variants of *APP*, *PSEN1*, *PSEN2*, *ADAM10*, and *TREM2*; (3) defined as rare variants by gnomAD (minor allele frequency <0.01) and carried by more than one index patient while not detected in controls; and/or (4) were reported in association with AD in previous studies. Primer information can be found in supplemental materials (Table S1).

SNP linkage analysis was performed by Plink under different heritability models. The Haploview program was used for analysis of Linkage Disequilibrium (LD) with the aim to identify haplotype blocks with significant association.

### ADNI database and related bioinformatics analysis

The Alzheimer's Disease Neuroimaging Initiative (ADNI) is a multisite longitudinal study, which aims to track the progression of AD with clinical, imaging, genetic, and biospecimen biomarkers, to validate biomarkers for use in AD clinical treatment trials. ADNI has had a global impact due to standardized protocols and its open data-sharing policy. Based on our findings, the Linux awk command was used to extract sequencing information for the *ACE* gene from sequencing of Chromosome 17. Gene annotation of extracted variants was performed by means of an online tool, wANNOVAR ([wannovar.wglab.org](http://wannovar.wglab.org)).<sup>23,25</sup> Corresponding clinical and imaging data (including information of family history) were collected according to the identifiers for selected individuals.

### Plasmid construction and cell culture, transfection

Wild type and mutant *ACE* plasmids were constructed by Sangon Biotech (Shanghai), respectively named *ACE*<sup>WT</sup>, *ACE* p.L1024fs and, for the truncating mutation, *ACE* p.1024X. An additional plasmid encoded the mutant Swedish APP (*APP*<sup>S<sup>W</sup></sup>), and the empty vector pcDNA3.1 was used as negative control. Human neuroblastoma SH-SY5Y cells were cultured into 6-well plates coated with poly-lysine and maintained in DMEM with 10% fetal bovine serum and penicillin-streptomycin (Gibco) in a 5% CO<sub>2</sub> incubator at 37°C. After cell density reached 70% confluence, co-transfection was performed using Lipofectamine 2000

(Invitrogen) according to the manufacturer's instructions. For each well, 1250 ng *APP*<sup>S<sup>W</sup></sup> plasmid DNA with 1250 ng *ACE*<sup>WT</sup>/*ACE* p.L1024fs/*ACE* p.L1024X plasmid DNA (Sangon Biotech) was mixed with Lipofectamine 2000, which was then added to the cells. 72 h after co-transfection, the culture media and cells were collected for further analysis.

### Western blot

After harvesting, cells were lysed with protein extraction reagent (with added Halt protease inhibitor cocktail, EDTA-Free) (ThermoFisher), and were subsequently centrifuged at 14,000 g for 10 min. Total protein was determined using the BCA Protein Assay Reagent (ThermoFisher). A total of 20 µg of denatured protein was loaded onto 10% SDS-PAGE gels. Once proteins were separated by electrophoresis, they were transferred to PVDF membranes (Immobilon-P<sup>SQ</sup>). After blocking in 5% nonfat milk for 2 h, the membranes were incubated with primary antibody (1:1000) overnight at 4°C. Then, membranes were washed with TBST for 3 times (10 min each) and incubated with species-matched peroxidase-conjugated secondary antibody (1:1000) for 2 h. The protein band was visualized by ECL (ThermoFisher). Images were captured, and band intensities were quantified using an Odyssey Image Station (LI-COR). The primary antibodies used in this study included anti-ACE antibody (Invitrogen, PA5-83080), anti-APP antibody (Abcam, ab32136) and anti-β-actin antibody (Sigma, A5441). The secondary antibodies included horseradish peroxidase-conjugated goat anti-mouse or anti-rabbit IgG (Beyotime, A0216 or A0208).

### Enzyme-linked immunosorbent assay (ELISA)

After collection 72 h following transfection, cell culture media was centrifugated at 300 g for 10 min to remove cellular debris. ACE was detected using sandwich ELISA kits (Multi Sciences) according to the manufacturer's protocol. Plates were read at 450 nm on a Synergy MX plate reader (Bio-Tek).

### Statistical analysis

Demographic analysis was conducted using SPSS Statistics v22.0 and independent-sample *t* tests and Chi-square tests were used for measurements and numeric/integer count data, respectively. In SNP analysis, different models were calculated, including an Allele Model, a Dominant Model, a Recessive Model and a Genotype Model, as well as application of the Chi-square test, Fisher's exact test, and logistic regression analysis. FDR correction by the Benjamini-Hochberg (BH) adjustment and also Bonferroni adjusted *p* values were calculated. Logistic regression analysis was also applied to haplotype analysis. Odds ratio (OR) and 95% confidence interval (95% CI) were calculated. The Clopper-Pearson Method was applied in 95% CI for mutant rates of genes. Results of *in vitro* experiments were analyzed by GraphPad Prism 7 and analysis of

variance (ANOVA) was used when comparing more than two groups. Statistical significance was defined as  $P < 0.05$ .

## Results

### Demographic characteristics and SNP analysis

A total of 90 probands from LOAD families and 101 cognitively normal elderly persons were recruited as participants of this study. The two cohorts were matched in age and gender. 66.7% of patients carried at least one *APOE*  $\epsilon 4$  allele, whereas only 13.9% of normal controls did (Table 1). Heterozygous  $\epsilon 4$  was estimated to confer risk for FLOAD with an OR of 12.08 (95% CI: 5.68–25.69), while homozygotes of  $\epsilon 4$  had an approximative risk (OR = 14.50, 95% CI: 3.01–69.97). *APOE*  $\epsilon 4$  allele frequency in the FLOAD cohort was significantly higher than in the control cohort (38.9% vs. 7.9%, OR = 8.31, 95%CI ranged from 4.29 to 16.08,  $P < 0.001$ ). SNP association analysis indicated that only *APOE* rs429358 was linked to FLOAD when taking the adjusted  $p$  value into consideration (Fig. S1). On the other hand, several haplotypes within *APP* and *BIN1* were found to confer genetic risk for AD in addition to *APOE*  $\epsilon 4$  (Fig. S2, Table S2).

### Genetic profiles of FLOAD

The most frequent variant was *CR1* rs116806486 (p. T173A), which was harbored by five (5.6%, 5/90, 95% CI ranged from 1.8% to 12.5%) probands simultaneously. Followed by variants of *TREM2*, detected in four (4.4%, 4/90, 95% CI ranged from 1.2% to 10.9%) index patients. The individual carrier of both p.A130V and p.H157Y SNPs had an earlier onset age and more aggressive cognitive decline. Moreover, p.H157Y was identified in a second proband. The novel *TREM2* variant (NM\_001271821: exon4: c.496G>A: p.V166M) was predicted to be deleterious by more than two predictive algorithms. A few missense variants within *ACE* were detected in both cohorts, which may superficially suggest no conferrence of risk for AD. However, three 'pathogenic' or 'likely pathogenic' mutations of *ACE* (*ACE* p.W343X, *ACE* p. D441fs, *ACE* p. L1024fs) graded according to ACMG guidelines were found in probands from different pedigrees (3.3%, 3/90, 95% CI ranged from 0.7% to 9.4%) (Table 2).

One rare coding variant of *PLD3* (NM\_001031696: exon7: c.489C>G: p.I163M) and a novel variant in *ADAM10* (NM\_001320570: exon13: c.1748A>G: p.Q583R) were also detected in our AD cohort. There was only one *PSEN2*

mutation in an individual with AD phenotype, p.H169N. Three other coding variants of *PSEN2* were carried by cognitive normal controls, including 2 novel variants (p.T128A and p.E322G) and one reported variant (p.G34S). No missense mutations were detected in *APP* nor *PSEN1* in our two cohorts, in addition to 7 synonymous and non-coding region (UTR) mutations (Table S3).

Because the mutations of *ACE* in the AD cohort are novel and account for the third highest frequency (3.3%), we next focused on revealing the phenotype and related function(s) of *ACE* mutation.

### Frameshifting and stop-gain mutations of *ACE*

We noticed that the 'pathogenic' and 'likely pathogenic' mutations based on ACMG guidelines were all located in *ACE*. No other frame-shift or stop-gain variant was detected. Since AD was the only common phenotype, we questioned whether these mutations were associated with AD risk. These mutations (*ACE* p.W343X, *ACE* p. D441fs, *ACE* p. L1024fs) were predicted to have deleterious effects on protein function(s) of the angiotensin I-converting enzyme, which is encoded by the *ACE* gene. Sequence length shortened as a result of altered downstream amino acid sequence and premature termination (Fig. 1A). However, cosegregation analysis had not been realized due to the lack of samples from affected relatives (Most of them had passed away due to the proband's advanced onset age, which is necessarily distinct from the affected relatives of EOAD of a relatively young age.) (Fig. 1B). Neuroimaging showed typical features of AD, such as medial temporal lobe atrophy (MTA, Fig. 1C), hypometabolism (Fig. 1D), and most importantly, abnormal A $\beta$  deposition (Fig. 2A). As depicted, the patient with *ACE* p.L1024fs (Patient 2) exhibited more extensive A $\beta$  plaques formation than the patient with *ACE* p. D441fs (Patient 1), which is reflected by a wider area of red color.

With the aim to ascertain whether the mutation altering the length of the *ACE* protein-coding sequence is a likely genetic risk factor of AD, we extracted relative genetic, clinical and imaging results from the ADNI database. One non-frameshifting insertion (*ACE* p.L18\_L19insPL) and three frameshifting variants (p.R149Lfs\*53; p.D1058Yfs\*15; p.S1238Pfs\*118) were annotated by wANNOVAR. The non-frameshifting insertion variant was excluded from further analysis as some normal carriers showed negative A $\beta$  deposition according to PET imaging. The corresponding three patients who harbored frameshifted variants of *ACE* not only progressed to dementia, but also presented with positive A $\beta$  deposition (Fig. 2B–D). Detailed information can be found in Table 3 and the patients' identifiers from ADNI are listed. Unfortunately, information of family history was absent due to mismatched identifiers (The three identifiers were absent in the file that recorded details of family history).

To summarize, a total of 6 patients who carried *ACE* frame-shift or stop-gain mutations were in their 70s, and manifested with LOAD independent of gender and *APOE*  $\epsilon 4$  status. These results suggest that frame-shift or stop-gain mutations in *ACE* might play a role in LOAD with evidence of abnormal A $\beta$  deposition featured by AD.

**Table 1** Demographics and *APOE* genotypes.

Group		AD (n = 90)	Control (n = 101)	p value
Age		74.03 $\pm$ 7.03	73.04 $\pm$ 8.31	0.373
Gender	Male	40 (44.4%)	40 (39.6%)	0.499
	Female	50 (55.6%)	61 (60.4%)	
MMSE		17.70 $\pm$ 8.57	29.10 $\pm$ 0.82	0.000
<i>APOE</i>	$\epsilon 4$ -/-	30 (33.3%)	87 (86.1%)	0.000
	$\epsilon 4$ +/-	50 (55.6%)	12 (11.9%)	
	$\epsilon 4$ +/+	10 (11.1%)	2 (2.0%)	

**Table 2** Mutation profiles and detailed information.

Gene	Exon	position	Ref/Alt	variant	Number of carriers	gnomAD_exome	gnomAD_gnome	Pathogenicity prediction				Reference
								SIFT	PolyPhen	MutationTaster	CADD	
<i>CR1</i> NM_000573	5	rs116806486	A/G	p.T173A	5	0.00158534	0.0053	T	B	N	0.001	Ma X.Y. et al (2014)
<i>TREM2</i> NM_018965	3	rs2234255	C/T	p.H157Y	2	0.00490461	0.001	D	D	N	23.1	Jiang T. et al (2016)
<i>TREM2</i> NM_018965	2	rs145080901	C/T	p.A105V	1	0.0000636274	0.00006372	D	D	N	24.2	Jin et al (2015)
<i>TREM2</i> NM_001271821	4	rs199795809	G/A	p.V166M	1	0.000234658	0.0002	D	B	D	11.75	Not reported
<i>TREM2</i> NM_018965	2	rs201280312	C/T	p.A130V	1	0.00000799853	NF	T	P	N	10.98	Jiao et al (2014)
<i>ACE</i> NM_000789	8	—	C/-	p.D441fs	1	0.00000398168	NF	NA	NA	NA	NA	Not reported
<i>ACE</i> NM_000789	20	—	CT/-	p.L1024fs	1	NF	0.00003184	NA	NA	NA	NA	Not reported
<i>ACE</i> NM_000789	7	rs200225958	G/A	p.W343X	1	0.00000796045	NF	NA	NA	A	36	Not reported
<i>PSEN2</i> NM_000447	7	rs533813519	C/A	p.H169N	1	0.00048	0.0002	D	B	D	31	Shi et al (2015)
<i>ADAM10</i> NM_001320570	13	rs141701612	A/G	p.Q583R	1	0.000103427	0.0006	T	B	N	8.753	Not reported
<i>PLD3</i> NM_001031696	7	rs200529365	C/G	p.I163M	1	0.000229557	0.00006373	D	P	N	22.7	Tan M.S. et al (2018)

Note: SIFT (D = damaging, T = tolerated); PolyPhen (B = benign, P = possibly damaging, D = probably damaging); Mutation Taster (A = disease\_causing\_automatic, D = disease\_causing, N = polymorphism, P = polymorphism\_automatic); NF = not found; NA = not available.



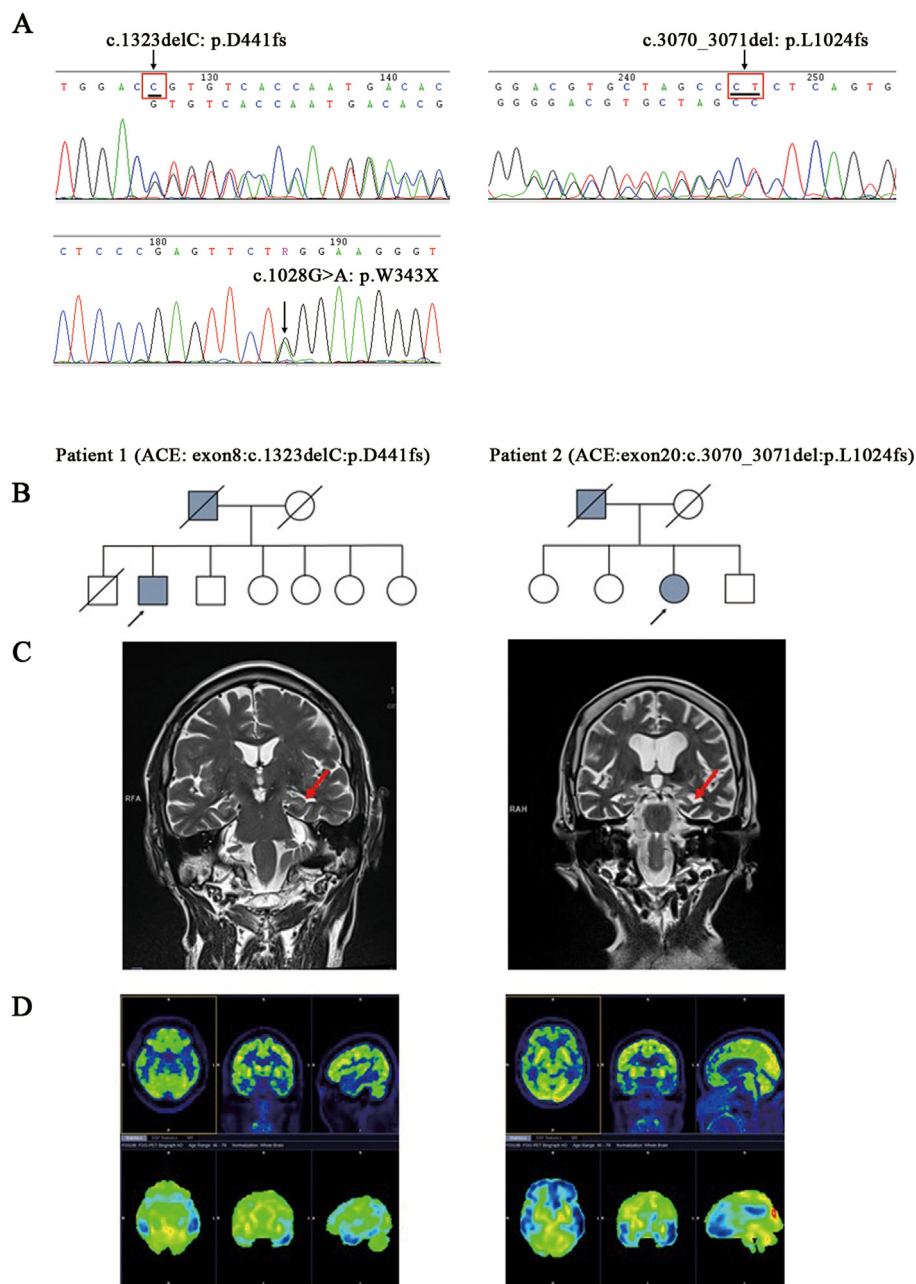


**Figure 1** Sanger Sequencing and clinical details of the index patients harboring *ACE* pathogenic mutations. **(A)** Verification of Sanger Sequencing for *ACE* frameshifting and stop-gain mutations. **(B–D)** The other index patient who carried *ACE* p.W343X was lost to follow-up. Patient 1: 74 years old, male, APOE  $\epsilon 2/\epsilon 3$ , MMSE 23/30 (education: 12 years); Patient 2: 74 years old, female, APOE  $\epsilon 3/\epsilon 4$ , MMSE 11/30 (education: 6 years). **(B)** Pedigrees with the index patient labeled by a black arrow. **(C)** Slices of coronal magnetic resonance imaging demonstrating hippocampal atrophy (red arrow). Patient 1: MTA = 3; Patient 2: MTA = 4. **(D)** Image of  $^{18}\text{F}$ -FDG PET shows reduced metabolism, especially in parietal, temporal, and frontal lobes.

### *ACE* mutation decreases *ACE* expression without influencing APP *in vitro*

As the significantly elevated  $\text{A}\beta$  deposition shown in the patient with *ACE* p.L1024fs, we further investigated whether this mutation influenced APP processing. In addition, we also constructed another truncating mutant plasmid (*ACE* p.L1024X) to compare to the frame-shifted construct and determine whether there could be a gain-of-function from

the shift of reading frames. Membrane-localized *ACE* protein was significantly decreased after transfection with *ACE* p.L1024fs compared to *ACE*<sup>WT</sup> (Fig. 3A, B), and was consistent with the decrease in secreted *ACE* in the cell culture medium (Fig. 3D). A similar tendency was also observed with transfection of the other construct for *ACE*, p.L1024X. Consistently, the expression of secreted *ACE* in samples transfected with *ACE* p.L1024fs was even lower compared to *ACE* p.L1024X (Fig. 3D), indicating that the frame-shift

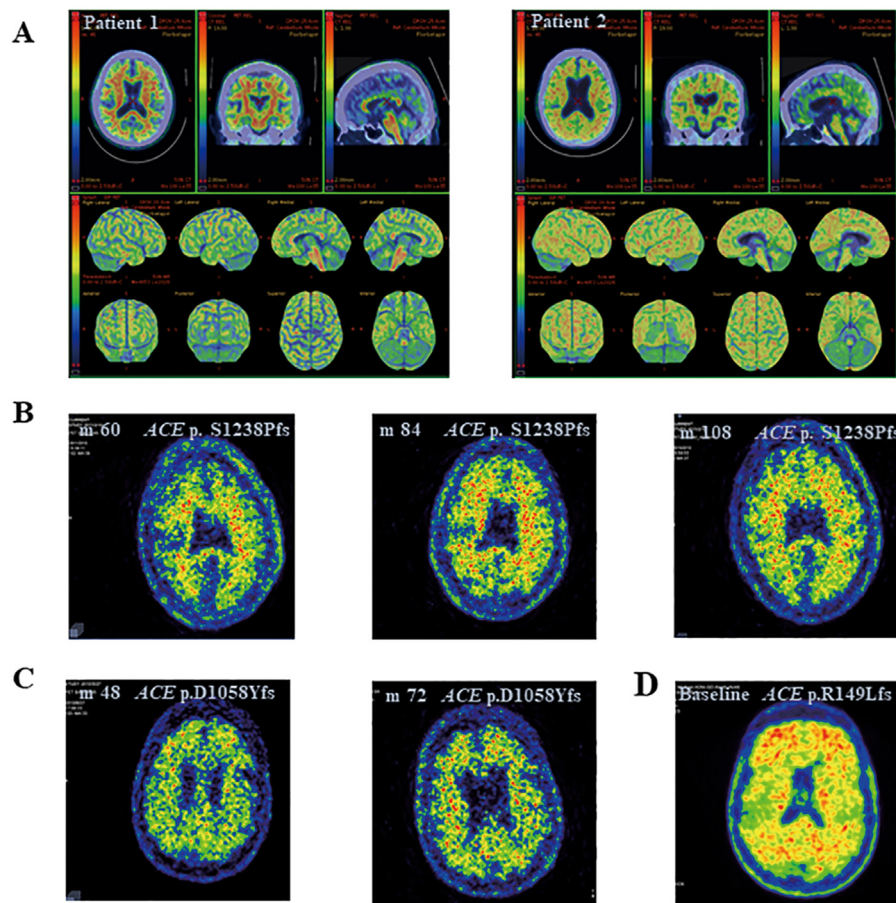


**Figure 2** 18F-AV-45 (18F-Florbetapir) PET imagings of patients with *ACE* frameshifting mutations. **(A)** Intracranial A $\beta$  deposition for Patient 1 and Patient 2 respectively: Transverse section, Coronal section, Medial sagittal section and 3-dimensional reconstruction models; **(B–D)** Intracranial A $\beta$  deposition for patients from ADNI and “m” represented follow-up months after baseline. As time progressed, more A $\beta$  deposited in the patients with *ACE* p. S1238Pfs (B) and *ACE* p.D1058Yfs (C). The last patient who harbored *ACE* p.R149Lfs had abundant A $\beta$  deposition at baseline (D). Warm color represents an increased uptake, which indicates abnormal A $\beta$  deposition.

mutation might have a more deleterious effect than the nonsense mutation at the same site. However, expression levels of full-length APP remained unchanged among the

cells transfected with *ACE*<sup>WT</sup>, *ACE* p.L1024fs, *ACE* p.L1024X and negative control (Fig. 3A, C). These results suggest that *ACE* p.L1024fs lowers expression of both membrane-

**Table 3** Clinical information of patients carried *ACE* frame-shifting or stop-gain mutations from our study and ADNI.

ADNI PTID	Bases variant	<i>ACE</i> mutation	Age (BL)	gender	RACE	diagnosis at baseline	AAO	duration to dementia (years)	<i>APOE</i> e4	AV-45-PET	MTA scale <sup>1</sup>
–	c.1323delC	p.D441fs	74	male	yellow	mild AD	72	2	0/0	(+)	3
–	c.3070_3071delCT	p.L1024fs	74	female	yellow	moderate AD	70	3	1/0	(+++)	4
–	c.1028G>A	p.W343X	71	male	yellow	moderate AD	NA	NA	1/0	NA	NA
068_S_2316	c.441_442insAGCTT	p.R149Lfs*53	74.3	female	white	early MCI	NA	1	1/0	(+++)	4
023_S_0887	c.3168_3181del	p.D1058Yfs*15	73.7	female	white	late MCI	NA	1.5	1/0	(++)	4
023_S_0061	c.3712delT	p.S1238Pfs*118	77	female	black	CN	79	6	0/0	(+++)	4

Note: AAO = age at onset; MTA = medial temporallobe atrophy;

<sup>1</sup> Scores based on the latest MRI.

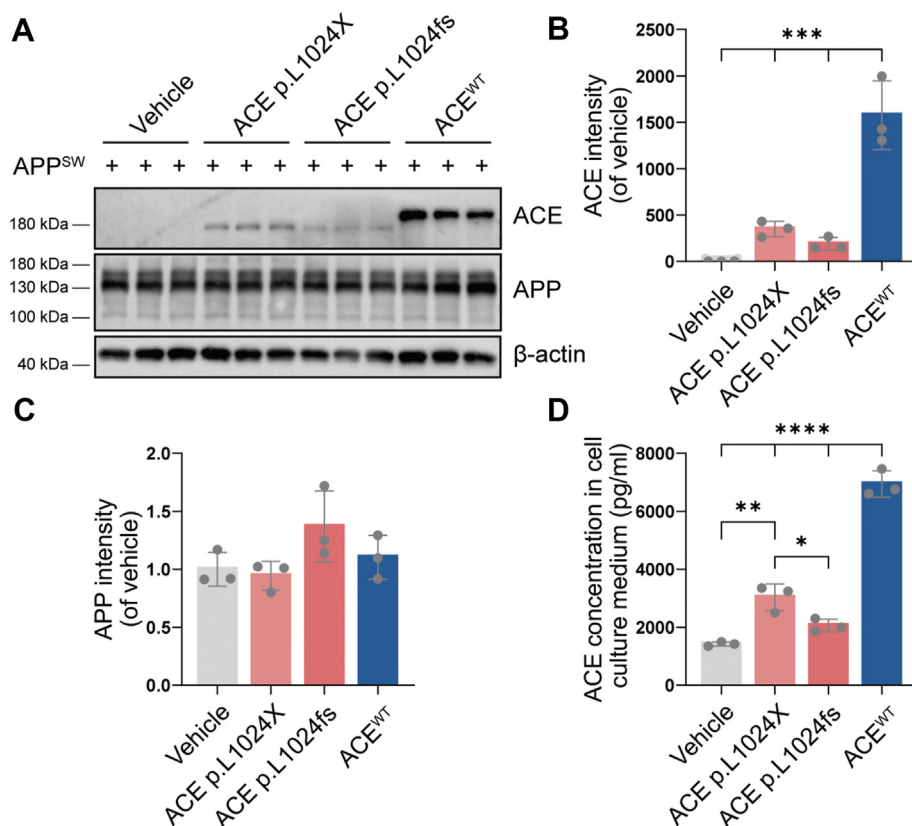


**Figure 3** Membrane-localized and secreted ACE change consistently, but expression of APP remains unchanged. (A) Expression of ACE and APP in SH-SY5Y cells co-transfected with APP<sup>SW</sup> and ACE<sup>WT</sup>/ACE p.L1024fs/ACE p.L1024X. (B, C) quantification of ACE and APP expression, respectively. (D) quantification of the secreted ACE in culture medium by ELISA after co-transfection.

localized and secreted ACE, but has no direct impact on APP processing.

## Discussion

This study is the first exploration of genetic screening for familial late-onset Alzheimer's Disease (FLOAD) to our knowledge. The frequency (66.7%) of APOE  $\epsilon$ 4 allele carriers in our FLOAD cohort is higher compared to that of sporadic AD in a prior Asian cohort (41.88%, 95%CI ranging from 38.48% to 45.27%)<sup>26</sup> and that of the Chinese Familial Alzheimer's Disease Network (CFAN) cohort (51.37%).<sup>4</sup>

The frequency (1.1%, 1/90) of APP, PSEN1, and PSEN2 missense mutations in our FLOAD cohort is significantly lower compared to previous studies of different ethnic populations. The major reason might be that only FLOAD was included in our study whereas a considerable proportion of familial EOAD were recruited in other studies. The only PSEN2 mutation (PSEN2 p.H169N) in the present case cohort was first discovered in a Chinese patient once before, and this individual was also phenotyped with FLOAD and amyloid deposition.<sup>27</sup> PSEN2 (p.G34S) was reported in Dutch LOAD patients and not observed in 283 healthy controls with unchanged A $\beta$ 42/A $\beta$ 40 ratio at the cellular level (unpublished data).<sup>28</sup> In our cohorts, G34S was detected in two controls, both of whom have no complaints about memory nor any cognitive decline. G34S seems benign rather than pathogenic based on these results. Similarly,

the other two novel variants (p.T128A and p.E322G) we found might be polymorphisms according to the algorithm proposed by Guerreiro and his colleagues.<sup>29</sup>

TREM2 and CR1, encoding triggering receptor expressed on myeloid cells 2 and complement receptor 1 protein, respectively, are involved in neuroinflammation and immune response related pathways.<sup>30,31</sup> A total of 10% of FLOAD probands carried variants of CR1 rs116806486 (5/90) or TREM2 (4/90) in our study, making the two genes notable among the candidates. On the one hand, the missense variant CR1 rs116806486 (p. T173A) was confirmed to be associated with LOAD in northern Han Chinese cohorts with an OR of 3.21 (95%CI: from 1.37 to 7.54).<sup>32</sup> Our study find that the frequency of CR1 rs116806486 is higher in FLOAD than sporadic LOAD (5.6% versus 1.9%). On the other hand, few missense mutations of TREM2 have been reported to confer genetic risk for LOAD, with one being R47H.<sup>11,12,33</sup> However, R47H-mediated increase in the risk for AD may be race-specific. This risk locus has only been reported in European and North American populations, but not in Asian populations.<sup>34</sup> Another TREM2 variant (p.H157Y) has been detected in Chinese populations and conferred considerable risk of LOAD with an OR of 11.01 (95% CI ranged from 1.38 to 88.05).<sup>35</sup> This position, histidine 157, is a cleavage site of TREM2. The p.H157Y variant results in enhanced shedding of TREM2, thus lowering TREM2-dependent phagocytosis.<sup>36</sup> Frequency of p.H157Y is higher in our FLOAD cohort (2.2%, 2/90) than that of previous sporadic



cases (0.8%, 8/988).<sup>35</sup> It seems that H157Y increasing the risk of LOAD is unique to the Chinese population, especially in FLOAD. The proband harboring two *TREM2* variants shows an earlier onset age and more aggressive progression, indicating that genetic risks may have an additive effect. These results highlight the role of complement-mediated and microglia-related innate immunity in LOAD.

Most importantly, this study is the first to find correlation between novel *ACE* frameshifting or nonsense mutations and AD. All six patients (three from our FLOAD cohorts, three from ADNI) were diagnosed with AD or onset in their seventies. *ACE* encodes the angiotensin I-converting enzyme (*ACE*), which converts angiotensin I to angiotensin II. It is a key component of the renin-angiotensin system (*RAS*), and is crucial in modulating blood pressure. Numerous preclinical and clinical studies have provided evidence supporting an association between *ACE* and AD, in addition to *ACE* identified as a risk gene by GWAS. On the one hand, increased *ACE* was found in AD brains, along with angiotensin II and AT1 receptor.<sup>37</sup> On the other hand, *ACE* protein level and activity in CSF and serum were decreased in AD patients compared to controls.<sup>38</sup> Results of clinical studies were contradictory. Some interpretations were that *ACE* inhibitors provided protection against AD onset and cognitive decline,<sup>39–42</sup> whereas others have found the opposite.<sup>43–46</sup> *In vitro* studies showed that *ACE* is involved in A $\beta$  degradation,<sup>47</sup> and the active center might be the N-terminal domain rather than the C-terminal domain.<sup>48</sup> Research within the past 12 years has indicated a potential AD treatment target could be *ACE* and has led to a proposed Angiotensin hypothesis of AD.<sup>49,50</sup> In a human APP transgenic mouse model, an effective dose of *ACE* inhibitor was found to be sufficient to promote formation of amyloid plaques. Moreover, heterozygous *ACE* deletion (*APP/ACE*<sup>+/-</sup>) led to a decline in *ACE* expression and accelerated A $\beta$ 42 deposition.<sup>45</sup> However, the mechanistic role of *ACE* and related pathways in the pathogenesis of AD remains undetermined. In the present study, our *in vitro* experiments suggest that frame-shift and nonsense *ACE* mutations resulted in decreased *ACE* protein levels. By contrast, recent research identified *ACE* rs4980 (R1279Q) as a penetrant mutation in AD and demonstrated elevated *ACE* levels, *ACE* activity and other *RAS* components in knock-in mice models, accelerating neurodegeneration and neuroinflammation independent of A $\beta$  pathology.<sup>51</sup> Although these results seem inconsistent, it is consistent with a role for either decreased or elevated *ACE* playing a role in AD risk through different mechanisms. In addition, *ACE2*, another *RAS* regulator which proteolytically activates angiotensin, was found to decrease amyloid pathology and provide a protective effect on cognitive decline.<sup>52</sup> Taken together, *ACE* and related *RAS* signaling are critical in AD with still incompletely understood, but intersecting, molecular pathways.

Limitations of this study include: (1) The probands recruited for this study are clinically diagnosed without a pathological diagnosis. (2) It is also a possibility that cognitively normal controls developed dementia in later years, and this has not been ruled out. (3) Furthermore, the absence of relatives' DNA samples makes it impossible to explore co-segregation of variants with AD. (4) Due to target sequencing, negative results in other probands do

not mean that there are no mutations in the undetected genes.

## Conclusions

In conclusion, we found genetic heterogeneity of FLOAD. Among the patients with FLOAD in China, *CR1* rs116806486 is the most frequent coding variant, followed by missense mutations in *TREM2* and pathogenic mutations in *ACE*. Combined with verification of data in the ADNI database, our study supports a hypothesis that frame-shift and nonsense mutations in *ACE* might contribute to the genetic etiology of LOAD. The imbalance of *RAS* caused by decreased *ACE* expression could be involved in pathogenic mechanism(s) of AD which will require further investigation to elucidate.

## Conflict of interests

The authors declare no competing interests.

## Funding

This work was funded by the Natural Science Foundation of China (No. 81671043, 81971068, 82071200), the Natural Science Foundation of Shanghai (No. 219ZR1431500), the Shanghai Municipal Education Commission-Gaofeng Clinical Medicine Grant (No. 20172001), the Shanghai Municipal Science and Technology Major Project (No. 2018SHZDZX01) and a Shanghai "Rising Stars of Medical Talent" Youth Development Program-Outstanding Youth Medical Talents Grant [2018].

Data collection and sharing for ADNI was funded by the Alzheimer's Disease Neuroimaging Initiative (National Institutes of Health Grant U01 AG024904) and DOD ADNI (Department of Defense award number W81XWH-12-2-0012). ADNI is funded by the National Institute on Aging, the National Institute of Biomedical Imaging and Bioengineering, and through generous contributions from the following: AbbVie, the Alzheimer's Association; the Alzheimer's Drug Discovery Foundation; Araclon Biotech; BioClinica, Inc.; Biogen; Bristol-Myers Squibb Company; CereSpir, Inc.; Cogstate; Eisai Inc.; Elan Pharmaceuticals, Inc.; Eli Lilly and Company; EuroImmun; F. Hoffmann-La Roche Ltd and its affiliated company Genentech, Inc.; Fujirebio; GE Healthcare; IXICO Ltd.; Janssen Alzheimer Immunotherapy Research & Development, LLC.; Johnson & Johnson Pharmaceutical Research & Development LLC.; Lumosity; Lundbeck; Merck & Co., Inc.; Meso Scale Diagnostics, LLC.; NeuroRx Research; Neurotrack Technologies; Novartis Pharmaceuticals Corporation; Pfizer Inc.; Piramal Imaging; Servier; Takeda Pharmaceutical Company; and Transition Therapeutics. The Canadian Institutes of Health Research is providing funds to support ADNI clinical sites in Canada. Private sector contributions are facilitated by the Foundation for the National Institutes of Health ([www.fnih.org](http://www.fnih.org)). The grantee organization is the Northern California Institute for Research and Education, and the study is coordinated by the Alzheimer's Therapeutic Research Institute at the University of

Southern California. ADNI data are disseminated by the Laboratory for Neuro Imaging at the University of Southern California.

## Acknowledgements

The authors sincerely thank all participants for their support. We thank Dr. Jin-Yan Huang, State Key Laboratory of Medical Genomics, Shanghai Institute of Hematology, National Research Center for Translational Medicine, Ruijin Hospital, Shanghai Jiao Tong University School of Medicine, for help in editing the Linux awk command for extracting sequence information for the ACE gene. We also thank Dr. Miao Zhang, Department of Nuclear Medicine, Ruijin Hospital, Shanghai Jiaotong University School of Medicine for visualizing raw imaging sequences of AV45-PET downloaded from ADNI.

## Appendix A. Supplementary data

Supplementary data to this article can be found online at <https://doi.org/10.1016/j.gendis.2021.05.001>.

## References

- Scheltens P, Blennow K, Breteler MM, et al. Alzheimer's disease. *Lancet*. 2016;388(10043):505–517.
- van der Flier WM, Pijnenburg YA, Fox NC, Scheltens P. Early-onset versus late-onset Alzheimer's disease: the case of the missing APOE  $\epsilon$ 4 allele. *Lancet Neurol*. 2011;10(3):280–288.
- Gao Y, Ren RJ, Zhong ZL, et al. Mutation profile of APP, PSEN1, and PSEN2 in Chinese familial Alzheimer's disease. *Neurobiol Aging*. 2019;77:154–157.
- Jia L, Fu Y, Shen L, et al. PSEN1, PSEN2, and APP mutations in 404 Chinese pedigrees with familial Alzheimer's disease. *Alzheimer's Dement*. 2020;16(1):178–191.
- Blauwendraat C, Wilke C, Jansen IE, et al. Pilot whole-exome sequencing of a German early-onset Alzheimer's disease cohort reveals a substantial frequency of PSEN2 variants. *Neurobiol Aging*. 2016;37:208.
- Mawuenyega KG, Sigurdson W, Ovod V, et al. Decreased clearance of CNS beta-amyloid in Alzheimer's disease. *Science*. 2010;330(6012):1774.
- Yamazaki Y, Zhao N, Caulfield TR, Liu CC, Bu G. Apolipoprotein E and Alzheimer disease: pathobiology and targeting strategies. *Nat Rev Neurol*. 2019;15(9):501–518.
- Neu SC, Pa J, Kukull W, et al. Apolipoprotein E genotype and sex risk factors for Alzheimer disease: a meta-analysis. *JAMA Neurol*. 2017;74(10):1178–1189.
- Belloy ME, Napolioni V, Greicius MD. A quarter century of APOE and Alzheimer's disease: progress to date and the path forward. *Neuron*. 2019;101(5):820–838.
- Kim M, Suh J, Romano D, et al. Potential late-onset Alzheimer's disease-associated mutations in the ADAM10 gene attenuate  $\{\alpha\}$ -secretase activity. *Hum Mol Genet*. 2009;18(20):3987–3996.
- Guerreiro R, Wojtas A, Bras J, et al. TREM2 variants in Alzheimer's disease. *N Engl J Med*. 2013;368(2):117–127.
- Jonsson T, Stefansson H, Steinberg S, et al. Variant of TREM2 associated with the risk of Alzheimer's disease. *N Engl J Med*. 2013;368(2):107–116.
- Cruchaga C, Karch CM, Jin SC, et al. Rare coding variants in the phospholipase D3 gene confer risk for Alzheimer's disease. *Nature*. 2014;505(7484):550–554.
- Lambert JC, Ibrahim-Verbaas CA, Harold D, et al. Meta-analysis of 74,046 individuals identifies 11 new susceptibility loci for Alzheimer's disease. *Nat Genet*. 2013;45(12):1452–1458.
- Kunkle BW, Grenier-Boley B, Sims R, et al. Genetic meta-analysis of diagnosed Alzheimer's disease identifies new risk loci and implicates A $\beta$ , tau, immunity and lipid processing. *Nat Genet*. 2019;51(3):414–430.
- Wijsman EM, Pankratz ND, Choi Y, et al. Genome-wide association of familial late-onset Alzheimer's disease replicates BIN1 and CLU and nominates CUGBP2 in interaction with APOE. *PLoS Genet*. 2011;7(2):e1001308.
- Marioni RE, Harris SE, Zhang Q, et al. GWAS on family history of Alzheimer's disease. *Transl Psychiatry*. 2018;8(1):99.
- Fernández MV, Budde J, Del-Aguila JL, et al. Evaluation of gene-based family-based methods to detect novel genes associated with familial late onset Alzheimer disease. *Front Neurosci*. 2018;12:209.
- Tosto G, Vardarajan B, Satriya S, et al. Association of variants in PINX1 and TREM2 with late-onset Alzheimer disease. *JAMA Neurol*. 2019;76(8):942–948.
- McKhann GM, Knopman DS, Chertkow H, et al. The diagnosis of dementia due to Alzheimer's disease: recommendations from the National Institute on Aging-Alzheimer's Association workgroups on diagnostic guidelines for Alzheimer's disease. *Alzheimer's Dement*. 2011;7(3):263–269.
- Li H, Durbin R. Fast and accurate long-read alignment with Burrows-Wheeler transform. *Bioinformatics*. 2010;26(5):589–595.
- McKenna A, Hanna M, Banks E, et al. The Genome Analysis Toolkit: a MapReduce framework for analyzing next-generation DNA sequencing data. *Genome Res*. 2010;20(9):1297–1303.
- Wang K, Li M, Hakonarson H. ANNOVAR: functional annotation of genetic variants from high-throughput sequencing data. *Nucleic Acids Res*. 2010;38(16):e164.
- Richards S, Aziz N, Bale S, et al. Standards and guidelines for the interpretation of sequence variants: a joint consensus recommendation of the American College of medical genetics and Genomics and the association for molecular pathology. *Genet Med*. 2015;17(5):405–424.
- Chang X, Wang K. wANNOVAR: annotating genetic variants for personal genomes via the web. *J Med Genet*. 2012;49(7):433–436.
- Ward A, Crean S, Mercaldi CJ, et al. Prevalence of apolipoprotein E4 genotype and homozygotes (APOE  $\epsilon$ 4/4) among patients diagnosed with Alzheimer's disease: a systematic review and meta-analysis. *Neuroepidemiology*. 2012;38(1):1–17.
- Shi Z, Wang Y, Liu S, et al. Clinical and neuroimaging characterization of Chinese dementia patients with PSEN1 and PSEN2 mutations. *Dement Geriatr Cognit Disord*. 2015;39(1–2):32–40.
- Sleegers K, Roks G, Theuns J, et al. Familial clustering and genetic risk for dementia in a genetically isolated Dutch population. *Brain*. 2004;127(Pt 7):1641–1649.
- Guerreiro RJ, Baquero M, Blesa R, et al. Genetic screening of Alzheimer's disease genes in Iberian and African samples yields novel mutations in presenilins and APP. *Neurobiol Aging*. 2010;31(5):725–731.
- Karch CM, Goate AM. Alzheimer's disease risk genes and mechanisms of disease pathogenesis. *Biol Psychiatr*. 2015;77(1):43–51.
- Kwon HS, Koh SH. Neuroinflammation in neurodegenerative disorders: the roles of microglia and astrocytes. *Transl Neurodegener*. 2020;9(1):42.
- Ma XY, Yu JT, Tan MS, Sun FR, Miao D, Tan L. Missense variants in CR1 are associated with increased risk of Alzheimer' disease in Han Chinese. *Neurobiol Aging*. 2014;35(2):443.

33. Sims R, van der Lee SJ, Naj AC, et al. Rare coding variants in *PLCG2*, *ABI3*, and *TREM2* implicate microglial-mediated innate immunity in Alzheimer's disease. *Nat Genet.* 2017;49(9):1373–1384.
34. Carmona S, Zahs K, Wu E, Dakin K, Bras J, Guerreiro R. The role of *TREM2* in Alzheimer's disease and other neurodegenerative disorders. *Lancet Neurol.* 2018;17(8):721–730.
35. Jiang T, Tan L, Chen Q, et al. A rare coding variant in *TREM2* increases risk for Alzheimer's disease in Han Chinese. *Neurobiol Aging.* 2016;42:217.
36. Schlepckow K, Kleinberger G, Fukumori A, et al. An Alzheimer-associated *TREM2* variant occurs at the ADAM cleavage site and affects shedding and phagocytic function. *EMBO Mol Med.* 2017;9(10):1356–1365.
37. Savaskan E, Hock C, Olivieri G, et al. Cortical alterations of angiotensin converting enzyme, angiotensin II and AT1 receptor in Alzheimer's dementia. *Neurobiol Aging.* 2001;22(4):541–546.
38. Jochimsen HM, Teunissen CE, Ashby EL, et al. The association of angiotensin-converting enzyme with biomarkers for Alzheimer's disease. *Alzheimer's Res Ther.* 2014;6(3):27.
39. Ohru T, Matsui T, Yamaya M, et al. Angiotensin-converting enzyme inhibitors and incidence of Alzheimer's disease in Japan. *J Am Geriatr Soc.* 2004;52(4):649–650.
40. Haag MD, Hofman A, Koudstaal PJ, Breteler MM, Stricker BH. Duration of antihypertensive drug use and risk of dementia: a prospective cohort study. *Neurology.* 2009;72(20):1727–1734.
41. Davies NM, Kehoe PG, Ben-Shlomo Y, Martin RM. Associations of anti-hypertensive treatments with Alzheimer's disease, vascular dementia, and other dementias. *J Alzheimers Dis.* 2011;26(4):699–708.
42. Birkenhäger WH, Staessen JA. Antihypertensives for prevention of Alzheimer's disease. *Lancet Neurol.* 2006;5(6):466–468.
43. Rosenberg PB, Mielke MM, Tschanz J, et al. Effects of cardiovascular medications on rate of functional decline in Alzheimer disease. *Am J Geriatr Psychiatry.* 2008;16(11):883–892.
44. Peters R, Beckett N, Forette F, et al. Incident dementia and blood pressure lowering in the Hypertension in the Very Elderly Trial cognitive function assessment (HYVET-COG): a double-blind, placebo controlled trial. *Lancet Neurol.* 2008;7(8):683–689.
45. Liu S, Ando F, Fujita Y, et al. A clinical dose of angiotensin-converting enzyme (ACE) inhibitor and heterozygous ACE deletion exacerbate Alzheimer's disease pathology in mice. *J Biol Chem.* 2019;294(25):9760–9770.
46. Hajjar I, Okafor M, McDaniel D, et al. Effects of Candesartan vs Lisinopril on neurocognitive function in older adults with executive mild cognitive impairment: a randomized clinical trial. *JAMA Netw Open.* 2020;3(8):e2012252.
47. Hemming ML, Selkoe DJ. Amyloid beta-protein is degraded by cellular angiotensin-converting enzyme (ACE) and elevated by an ACE inhibitor. *J Biol Chem.* 2005;280(45):37644–37650.
48. Oba R, Igarashi A, Kamata M, Nagata K, Takano S, Nakagawa H. The N-terminal active centre of human angiotensin-converting enzyme degrades Alzheimer amyloid beta-peptide. *Eur J Neurosci.* 2005;21(3):733–740.
49. Zou K, Michikawa M. Angiotensin-converting enzyme as a potential target for treatment of Alzheimer's disease: inhibition or activation? *Rev Neurosci.* 2008;19(4–5):203–212.
50. Kehoe PG. The coming of age of the angiotensin hypothesis in Alzheimer's disease: progress toward disease prevention and treatment? *J Alzheimers Dis.* 2018;62(3):1443–1466.
51. Cuddy LK, Prokopenko D, Cunningham EP, et al. A $\beta$ -accelerated neurodegeneration caused by Alzheimer's-associated ACE variant R1279Q is rescued by angiotensin system inhibition in mice. *Sci Transl Med.* 2020;12(563):eaaz2541.
52. Evans CE, Miners JS, Piva G, et al. ACE2 activation protects against cognitive decline and reduces amyloid pathology in the Tg2576 mouse model of Alzheimer's disease. *Acta Neuropathol.* 2020;139(3):485–502.